RESEARCH ARTICLE

Influence of Current-Dependent AC Resistance and Emissivity on Temperature Estimation of a Single-Layer ACSR Conductor

Miloš J. Milovanović[1,*], **Andrijana D. Jovanović**[1] **and Bojan D. Perović**[1]

[1] Faculty of Technical Sciences, University of Priština in Kosovska Mitrovica, RS-38220 Kosovska Mitrovica, Serbia

Abstract

This paper investigates the influence of temperature- and current-dependent variations in alternating current (AC) resistance on the estimation of the operating temperature of aluminium conductor steel-reinforced (ACSR) conductors, with particular emphasis on the differences arising from the use of tabulated and experimentally determined resistance characteristics. Special attention is devoted to the current dependence of AC resistance in the single-layer ACSR conductor 48-AL1/8-ST1A, where pronounced resistance variations occur due to the electromagnetic interaction between the aluminum strands and the steel core. Experimental investigations were conducted under controlled laboratory conditions using a dedicated measurement system capable of the synchronized acquisition of electrical and thermal quantities in real time. Based on the obtained measurements, AC resistance characteristics were determined as functions of both conductor temperature and current, and their influence on conductor temperature estimation was subsequently evaluated. The results demonstrate that neglecting the current dependence of AC resistance may lead to conductor temperature estimation errors of up to approximately 2.5 °C under current loadings close to the rated value, indicating that this effect should not be disregarded in thermal analyses of single-layer ACSR conductors. However, the study also reveals that conductor emissivity has a substantially larger influence on temperature estimation. Specifically, varying the assumed conductor surface emissivity from 0.3 to 0.9 results in calculated conductor temperature differences exceeding 15 °C, significantly outweighing the influence of current-dependent AC resistance. The obtained findings indicate that accurate determination of conductor emissivity is essential for reliable thermal analysis and Dynamic Line Rating (DLR) applications, while the use of experimentally determined AC resistance characteristics further improves the accuracy of conductor temperature and ampacity assessments.

Keywords: alternating current (AC) resistance, aluminum conductor steel-reinforced (ACSR) conductor, dynamic line rating (DLR), conductor emissivity.

Submitted: 03 June 2026
Revised: 21 July 2026
Accepted: 22 July 2026
Published: 03 August 2026

Vol. 2, **No.** 3, 2026.
10.62762/TEPNS.2026.632689

***Corresponding author:**
Miloš J. Milovanović
milos.milovanovic@pr.ac.rs

Citation
Milovanović, M. J., Jovanović, A. D., & Perović, B. D. (2026). Influence of Current-Dependent AC Resistance and Emissivity on Temperature Estimation of a Single-Layer ACSR Conductor. *ICCK Transactions on Electric Power Networks and Systems*, 2(3), 116–127.

1 Introduction

Overhead transmission lines (OTLs) constitute one of the fundamental components of power systems, while their power transfer capability is largely constrained by the thermal state of phase conductors. Conductor temperature directly affects mechanical stress, conductor sag, safety clearances, material aging, electrical losses, and the overall reliability of line operation [1, 2]. Therefore, accurate determination of conductor temperature is of paramount importance not only for the conventional planning and operation of OTLs but also for modern grid-management approaches aimed at maximizing the utilization of existing power system infrastructure [3, 4].

The thermal behavior of OTL conductors is commonly described by a heat balance equation, which establishes equilibrium between the heat generated within the conductor and the heat dissipated to the surrounding environment. The primary heat source is Joule heating, which depends on the square of the current and the alternating current (AC) resistance of the conductor. In stranded aluminum conductor steel-reinforced (ACSR) conductors, the AC resistance is influenced not only by temperature but also by complex electromagnetic phenomena, including skin effect, current redistribution between layers, and magnetic effects associated with the steel core [5]. Additional heat input may arise from solar radiation, whereas conductor cooling is achieved through convective and radiative heat transfer mechanisms. Methodologies for calculating conductor temperature and ampacity of bare OTL conductors are defined in IEEE Std 738 [6], CIGRÉ TB 601 [7], and IEC/TR 61597 [8]. Although these approaches are based on the same fundamental heat balance principle, their accuracy is strongly influenced by the representation of electrical resistance, conductor surface properties, and heat-transfer processes between the conductor and the surrounding environment.

A particularly important parameter in thermal rating calculations is the AC resistance of the conductor, since it directly affects heat generation within the conductor. Previous studies have highlighted that accurate determination of AC resistance is essential for the development of reliable Dynamic Line Rating (DLR) methodologies, since ohmic losses represent the dominant heat source affecting conductor temperature [2, 9]. In engineering practice and in most commonly used thermal rating models, AC resistance is treated as a known input parameter obtained from tabulated data or estimated through temperature-dependent correction relationships. Such an approach may be adequate for homogeneous stranded conductors, for which the influence of electromagnetic effects is relatively limited. However, the situation is considerably more complex in ACSR conductors owing to the presence of electromagnetic phenomena associated with the steel core [5]. For example, IEEE Std 738 [6] determines AC resistance using tabulated values specified at two reference temperatures, with intermediate values obtained through linear interpolation. These tabulated values are assumed to incorporate the effects of skin effect, conductor stranding, and, for certain ACSR constructions, magnetic phenomena associated with the steel core. Although this approach is practical for engineering applications, the standard acknowledges the limitations of linear interpolation outside the reference temperature range. Furthermore, it notes that magnetic effects in the steel core may increase the effective resistance of single-layer ACSR conductors by up to approximately 20% at high current levels [2, 9–12].

A similar assumption is adopted in most DLR methodologies, where Joule losses are calculated as a function of AC resistance and current squared, while the resistance itself is commonly obtained from tabulated data, manufacturer specifications, or simple temperature-dependent relationships. However, for ACSR conductors, such an approach may be insufficient because AC resistance is influenced not only by temperature but also by current-dependent electromagnetic phenomena [5]. Previous studies have shown that transformer effects associated with steel-core magnetization can introduce a pronounced current dependence of AC resistance, while the accurate calculation of this parameter remains particularly challenging for helically stranded conductors with magnetic cores [2, 5, 9, 10]. Consequently, inaccuracies in AC resistance modelling may directly affect conductor temperature estimation, ampacity calculations, and the overall accuracy of DLR assessments. The physical mechanisms responsible for the current dependence of AC resistance in ACSR conductors have been extensively investigated in the literature. Morgan [11] demonstrated that AC currents flowing through helically stranded aluminum layers generate an axial magnetic flux within the steel core, resulting in additional hysteresis and eddy-current losses as well as current redistribution between conductor layers. These phenomena, commonly referred to as transformer effects, increase the effective

AC resistance of the conductor. Similar conclusions were reported by Meyberg et al. [10], who showed that magnetic-core effects influence AC resistance and radial temperature distribution within ACSR conductors, particularly for conductor designs with an odd number of aluminum layers.

Recent studies have emphasized the importance of experimentally determining AC resistance for DLR applications. Riba et al. [9, 12] highlighted that the current dependence of AC resistance is generally neglected in conventional DLR methodologies, although it may significantly affect the estimation of conductor losses and thermal behavior. Furthermore, Xie et al. [13] pointed out that a universally accepted and standardized procedure specifically for AC resistance measurements of OTL conductors under actual operating conditions is still lacking and proposed an experimental approach for simultaneous investigation of conductor current, temperature, and AC resistance under operating conditions.

Despite these advances, most existing studies focus primarily on the characterization of AC resistance itself, while relatively little attention has been devoted to quantifying how the use of experimentally determined current-dependent AC resistance influences conductor temperature calculations. In addition, the effect of AC resistance modelling assumptions is rarely compared with other important thermal-rating parameters, such as conductor surface emissivity, which directly affects radiative cooling and may vary significantly depending on conductor age, oxidation level, contamination, and environmental exposure. Experimental investigations have shown that emissivity-related uncertainties may lead to substantial deviations in conductor temperature estimation and current-carrying capacity calculations; consequently, emissivity is considered one of the key parameters affecting the accuracy of thermal rating assessments [2, 6, 14].

Therefore, the objective of this paper is to investigate the influence of current-dependent AC resistance and conductor emissivity on the temperature estimation of the single-layer ACSR conductor 48-AL1/8-ST1A. Experimental investigations were performed under controlled laboratory conditions using a dedicated measurement system based on the NI CompactDAQ platform and LabVIEW environment, enabling the synchronized acquisition of electrical and thermal quantities [15]. Based on the measured current, voltage drop, phase angle, and conductor temperature, AC resistance characteristics were determined as functions of both conductor temperature and current. The experimentally obtained AC resistance characteristics were subsequently incorporated into conductor thermal calculations and compared with conventional approaches based on tabulated resistance values. Particular attention was devoted to quantifying the temperature estimation error associated with neglecting the current dependence of AC resistance. In addition, the influence of AC resistance modelling was directly compared with the influence of conductor emissivity in order to evaluate the relative importance of electrical and surface-related parameters in thermal rating calculations.

The main contribution of this work is the experimental quantification of the effect of current-dependent AC resistance on conductor temperature estimation and its direct comparison with the effect of conductor surface emissivity. Such a comparison provides a quantitative assessment of the relative importance of electrical and surface-related parameters in conductor thermal rating calculations and DLR applications. Furthermore, by evaluating both factors within the same experimental framework and under identical operating conditions, the proposed approach offers additional insight beyond what is achievable through separate or independent investigations.

2 Experimental Setup

This section presents the materials, measurement equipment, and experimental setup used in the laboratory investigations. The experiments were conducted on an ACSR conductor of type 48-AL1/8-ST1A, consisting of six aluminum strands helically wound around a central steel core strand. The conductor has a DC resistance of 0.5939 Ω/km at 20 °C and a continuous current-carrying capacity of 210 A under standard operating conditions. Owing to its single-layer stranded construction, this conductor exhibits a pronounced influence of current redistribution and magnetic effects associated with the steel core, making it particularly suitable for investigating the variation of AC resistance with conductor temperature and load current.

The test transformer represented a key component of the experimental setup, as it enabled the generation of high-current operating conditions that cannot be achieved using conventional laboratory power supplies, thereby allowing the thermal and electrical behavior of the conductor to be investigated under conditions representative of practical OTL operation.

Figure 1. Overview of the experimental setup used for AC resistance and thermal measurements of the investigated ACSR conductor: (1) variable autotransformer, (2) step-down transformer, (3) ACSR conductor, (4) current probe, (5) NI-9215 module, (6) NI cDAQ-9133 data acquisition chassis, (7) laptop with external monitor, (8) temperature sensors, (9) anemometer, (10) support insulator, and (11) fan.

The current source consisted of two single-phase transformers connected in cascade. A variable autotransformer (10 kVA, 0–230 V) was used to continuously regulate the input voltage of a step-down transformer (10 kVA, 230/5 V/V). The investigated ACSR conductor was connected to the secondary side of the step-down transformer, forming a low-impedance current loop, as illustrated in Figure 1. The total length of the test conductor was 8 m. To minimize the influence of contact resistance on the measurement results, the conductor ends were terminated using compression cable lugs, thereby ensuring reliable electrical connections and uniform current distribution throughout the test circuit.

The conductor current was measured using a Fluke i430-Flexi-TF-II flexible current probe, featuring a measurement range of 0–6 kA, a sensitivity of 85 mV at 1000 A (50 Hz), a linearity of $\pm 0.2\%$, and an accuracy of $\pm 0.5\%$ over the range from 5 A to 6 kA. The probe output was acquired using an NI-9215 data acquisition module integrated into an NI cDAQ-9133 measurement system. The NI-9215 provides four simultaneously sampled analog input channels with 16-bit resolution and a maximum sampling rate of 100 kS/s per channel, allowing synchronized acquisition of current and voltage signals required for the determination of conductor AC resistance.

The temperatures of the conductor surface and the ambient air were measured using Pt100 resistance temperature detectors (RTDs) (Class A, accuracy

$\pm(0.15 + 0.002|t|)$ °C) connected in a three-wire configuration to an NI-9217 temperature input module. The module provides four analog input channels and a measurement accuracy of ± 0.5 °C over the temperature range from -200 °C to 150 °C. To ensure good thermal contact between the sensor and the conductor surface, a thermally conductive paste was applied at the interface. The sensor was additionally secured to the conductor using a stainless-steel clamp. To minimize the influence of wind on the temperature measurements, the sensor assembly was covered with a self-adhesive aluminum tape, which provided both mechanical protection and shielding from direct airflow.

Data acquisition, processing, and real-time analysis were performed using LabVIEW 2024 software. Configuration and control of the measurement system were implemented through a custom-developed LabVIEW virtual instrument (VI), which enabled automated acquisition of voltage, current, and temperature data from the NI-9215 and NI-9217 modules integrated within the NI cDAQ-9133 data acquisition system. The developed software interface also provided real-time visualization, storage, and post-processing of the measured data, ensuring efficient monitoring of the experimental procedure and reliable determination of conductor resistance.

2.1 AC Resistance Determination

In accordance with the recommendations of CIGRÉ TB 345 [5], the AC resistance of the conductor was determined by separating the real component of the measured impedance rather than by direct resistance measurement. When an AC current I flows through the conductor, the measured voltage drop ΔU contains both resistive and reactive components. The in-phase component $\Delta U \cos\varphi$ is associated with the conductor resistance, whereas the quadrature component $\Delta U \sin\varphi$ is associated with the conductor reactance.

The AC resistance per unit length, R_{ac} (Ω/m), was calculated as:

$$R_{ac} = \frac{\Delta U}{I \cdot \ell} \cos\varphi \tag{1}$$

where ΔU is the measured voltage drop, I is the conductor current, φ is the phase angle between voltage and current, and ℓ is the length of the conductor segment over which the voltage drop was measured. This approach enables accurate extraction of the real component of impedance and reliable determination of AC resistance even in the presence of inductive and magnetic effects associated with the steel core of ACSR conductors.

The experimentally determined AC resistance was subsequently expressed as a function of conductor temperature. For the investigated temperature range, the dependence of AC resistance on temperature was approximated using a linear relationship:

$$R_{ac}(T) = R_{ac,0}\left[1 + \alpha_{ac}(T - T_0)\right] \tag{2}$$

where $R_{ac,0}$ is the AC resistance at the reference temperature T_0 (typically 20 °C), and α_{ac} is the temperature coefficient of AC resistance in °C^{-1}. The parameters $R_{ac,0}$ and α_{ac} were determined by applying linear regression to the experimentally obtained R_{ac}-versus-temperature characteristics for each investigated current level.

In standard thermal models [6–8], the selection of conductor electrical resistance is of fundamental importance. While the DC resistance (R_{dc}) is determined by the conductor geometry, material properties, and temperature, the AC resistance additionally depends on the operating frequency and the current distribution within the conductor. According to the recommendations of CIGRÉ TB 345 [5], the ratio between AC and DC resistance for single- and two-layer ACSR conductors is determined as:

$$\frac{R_{ac}}{R_{dc}} = 1.0045 + 0.09 \times 10^{-6} I_{ac} \tag{3}$$

where I_{ac} is the AC conductor current (in amperes). It should be noted that this relationship is applicable to single- and two-layer ACSR conductors, and is used in the present study as a reference baseline for comparison with the experimentally determined AC resistance characteristics.

As the current increases, the current distribution within the conductor cross-section becomes increasingly non-uniform due to the skin effect, while additional hysteresis and eddy-current losses develop in the steel core. This phenomenon, commonly referred to as the transformer effect, is caused by the AC magnetic field generated by the current flowing through the surrounding aluminum strands. Since conductor electrical resistance directly determines the magnitude of Joule heating in the

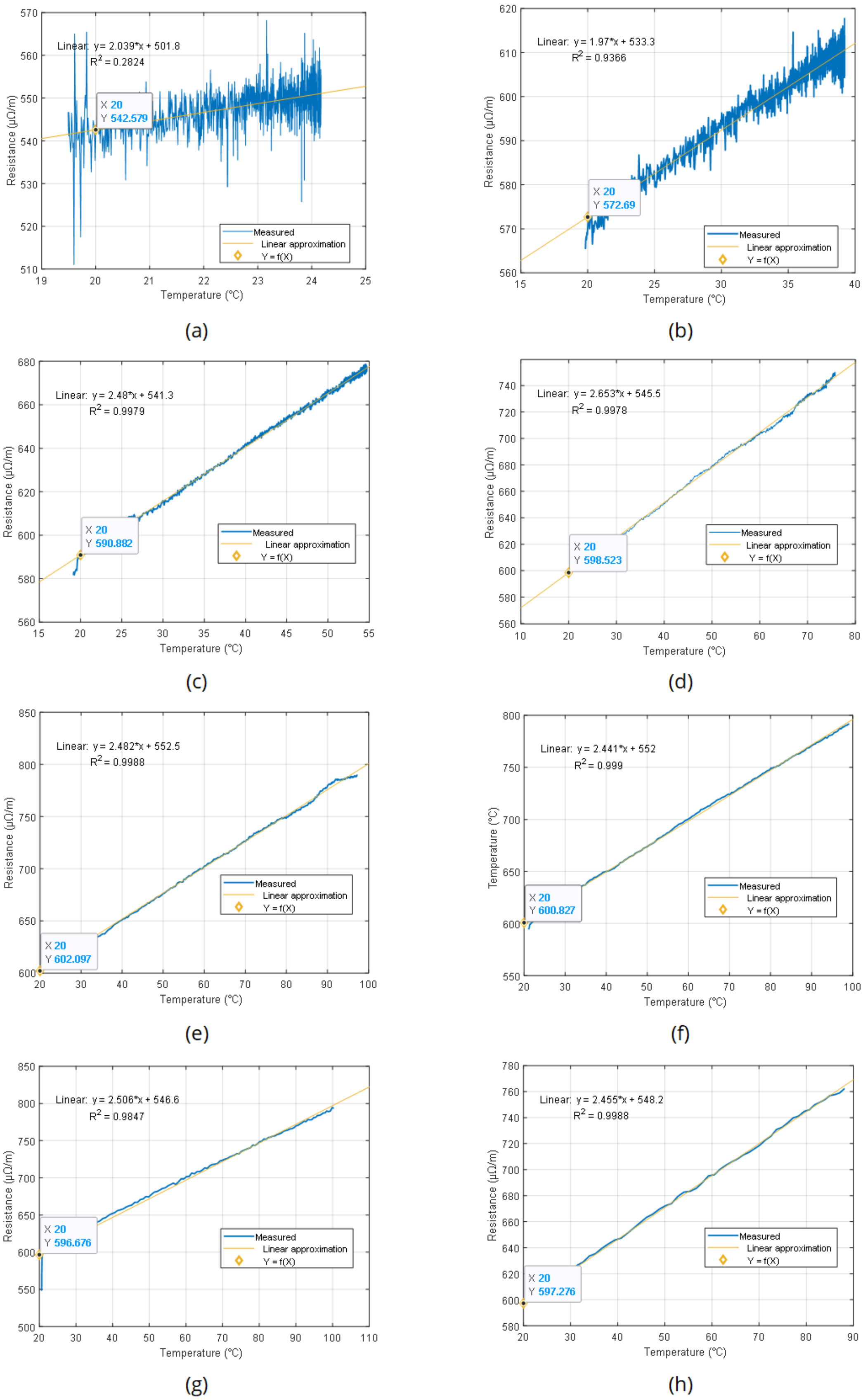

Figure 2. AC resistance–temperature characteristics of the 48-AL1/8-ST1A ACSR conductor obtained during the heating cycle for selected current levels of approximately: (a) 50 A, (b) 100 A, (c) 150 A, (d) 200 A, (e) 250 A, (f) 300 A, (g) 350 A, and (h) 400 A.

thermal balance equation, accurate representation of AC resistance is essential for reliable conductor temperature calculations. Consequently, the use of R_{dc} instead of R_{ac} may lead to an underestimation of conductor temperature, particularly under high-current operating conditions. In the present study, the influence of the current-dependent variation of resistance on the calculated temperature was investigated by comparing thermal model predictions obtained using the conventional temperature-dependent resistance model, $R = f(T)$, and the proposed current- and temperature-dependent model, $R = f(T, I)$.

2.2 Experimental Procedure

The experiments were performed at several prescribed current levels ranging from approximately $0.25 \cdot I_n$ to $2 \cdot I_n$ (50 A, 100 A, 150 A, 200 A, 250 A, 300 A, 350 A, and 400 A). Due to the constant-voltage supply and the increase in conductor temperature during the tests, the actual current gradually decreased as the conductor resistance increased. Therefore, all subsequent analyses were based on the measured steady-state current values rather than the initially prescribed current levels. For each current level, the conductor surface temperature was continuously measured at three locations along the test section. Simultaneously, the voltage drop over a 1 m conductor segment, conductor current, and phase angle between voltage and current were recorded. The AC resistance was then determined according to Eq. (1).

The investigated ACSR conductor, type 48-AL1/8-ST1A, has a rated current-carrying capacity of 210 A. For current levels exceeding the rated current, conductor temperatures in the range of approximately 80–100 °C were observed. Consequently, the test was terminated whenever this temperature threshold was reached in order to prevent thermal damage to the conductor. The obtained results were subsequently used to construct the AC resistance-temperature characteristics, $R_{ac} = f(I)$. Linear regression was applied to each dataset to determine the AC resistance at the reference temperature, $R_{ac,20}$, and the corresponding temperature coefficient, α_{ac}.

3 Results and Discussion

3.1 AC Resistance–Temperature Characteristics

Figure 2 presents the experimentally determined AC resistance-temperature characteristics of the investigated 48-AL1/8-ST1A conductor for current levels ranging from 50 A to 400 A. For all investigated operating conditions, the measured data exhibit a nearly linear dependence of AC resistance on conductor temperature. Except for the two lowest current levels (50 A and 100 A), the obtained values of the temperature coefficient remain nearly constant, ranging from approximately 0.0040 to 0.0044 $^{\circ}C^{-1}$, indicating that the temperature coefficient is practically independent of the operating current over the investigated range. In contrast, a more pronounced variation is observed for the reference AC resistance at 20 °C. The obtained values increase from 542.6 $\mu\Omega/m$ at 50 A to a maximum of 602.1 $\mu\Omega/m$ at 250 A, after which they slightly decrease to approximately 597 $\mu\Omega/m$ at the highest investigated current levels.

For clarity, the variation of the reference AC resistance with conductor current is presented separately in Figure 3 together with the tabulated DC resistance at the reference temperature. It can be observed that the experimentally determined reference AC resistance increases rapidly with increasing current and becomes equal to the tabulated DC resistance of 593.9 $\mu\Omega/m$ at approximately 145 A. Beyond this point, the reference AC resistance exceeds the DC value, reaching a maximum of approximately 602 $\mu\Omega/m$ at around 250 A, after which it exhibits a slight decrease toward an approximately constant value. The resulting current dependence exhibits a characteristic sigmoidal shape, rising steeply at intermediate current levels and approaching a plateau at higher currents. At lower current levels, the magnetic flux density in the steel core is relatively low and the transformer effect is weak. As the current increases, the magnetic flux density in the steel core rises, intensifying the transformer effect and increasing hysteresis and eddy-current losses. Consequently, the effective AC resistance increases. At higher current levels, the steel core gradually approaches magnetic saturation, reducing the rate of increase of the magnetic flux density and consequently weakening the transformer effect. As a result, the reference AC resistance reaches a maximum and then decreases slightly toward an approximately constant value.

To verify whether the observed current dependence of AC resistance could be attributed to the classical skin effect, its contribution was estimated according to the methodology given in CIGRÉ TB 345 [5]. For the investigated 48-AL1/8-ST1A conductor at 50 Hz, the skin effect increased the conductor resistance by only approximately 0.0054%. This confirms that the observed current-dependent variation of AC resistance is predominantly associated with the transformer effect

Table 1. Measured operating conditions, experimentally determined conductor parameters, and calculated conductor temperatures for the 48-AL1/8-ST1A conductor.

Calculation method	Measured operating conditions and conductor parameters				
Measured operating conditions and experimentally determined conductor parameters	Mean current, I_{mean} (A)	53.39	105.16	141.56	181.46
	Ambient temperature, T_a (°C)	19.75	20.13	19.97	19.98
	Reference AC resistance at 20 °C, $R_{ac,20}$ ($\mu\Omega$/m)	542.58	572.69	590.88	598.52
	Temperature coefficient of AC resistance, α_{ac} (1/°C)	0.0038	0.0035	0.0042	0.0044
	Measured conductor temperature, T_c (°C)	24.06	38.99	54.46	75.33
CIGRÉ TB 601 & IEEE Std 738, $R = f(T)$	Conductor temperature, T_c (°C)	25.40	39.20	53.00	73.00
CIGRÉ TB 601 & IEEE Std 738, $R = f(T,I)$		24.90	38.40	53.00	74.40

and magnetic losses in the steel core. This finding is consistent with the illustrative example provided for the single-layer Grackle ACSR conductor in Appendix C of CIGRÉ TB 345, where the skin-effect contribution also remains practically constant over the investigated current range.

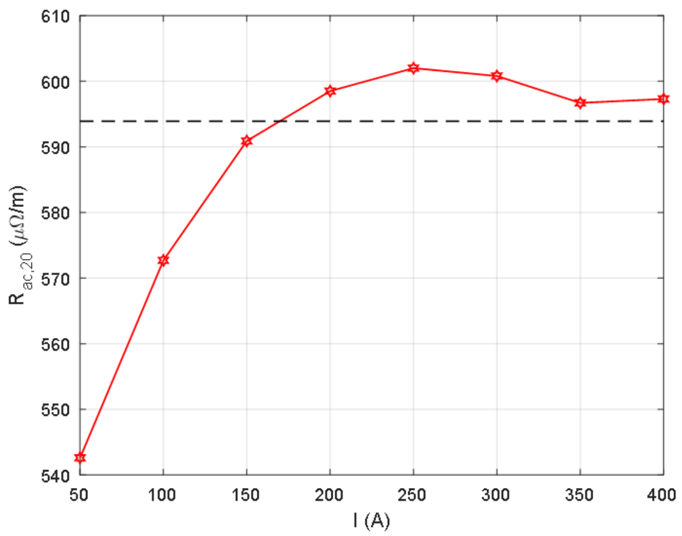

Figure 3. Current dependence of the experimentally determined reference AC resistance at 20°C for the investigated 48-AL1/8-ST1A ACSR conductor. The dashed line indicates the tabulated DC resistance.

To assess the reliability of the experimentally determined AC resistance values, a measurement uncertainty analysis was performed in accordance with the Guide to the Expression of Uncertainty in Measurement (GUM) [16]. The uncertainty evaluation considered the voltage measurement, current measurement, and phase-angle determination, while the combined standard uncertainty was evaluated using the law of propagation of uncertainty. The same uncertainty evaluation procedure was applied to all investigated operating points. The expanded measurement uncertainty (coverage factor $k = 2$, corresponding to approximately 95% confidence) remained below 2% of the corresponding measured AC resistance for all investigated operating points, confirming the reliability of the experimentally determined AC resistance characteristics and the reported results.

3.2 Influence of Current-Dependent AC Resistance on Conductor Temperature Estimation

The experimentally determined current dependence of AC resistance demonstrated in the previous section indicates that the conventional assumption of temperature-dependent resistance alone may not adequately represent the electrical behavior of single-layer ACSR conductors. Therefore, this section evaluates the influence of experimentally determined current-dependent AC resistance on conductor temperature estimation by comparing the conventional approach based on temperature-dependent resistance, $R = f(T)$, with the proposed current- and temperature-dependent resistance model, $R = f(T, I)$. The conductor surface emissivity was adopted to be 0.51, corresponding to the experimentally determined value for the investigated 48-AL1/8-ST1A conductor reported in [2]. The methodology used for emissivity identification is presented in detail in [2] and is therefore not repeated here. For the conventional temperature-dependent resistance model, $R = f(T)$, the calculations were performed using the tabulated DC resistance at 20 °C (593.9 $\mu\Omega$/m) together with a representative temperature coefficient of resistance of 0.0039 °C^{-1}, which lies within the range commonly reported for ACSR conductors [7]. In contrast, the proposed $R = f(T, I)$ model employs the experimentally determined reference AC resistance and the corresponding temperature coefficient obtained for each investigated operating condition.

The analysis was performed using both the CIGRÉ TB 601 [7] and IEEE Std 738 [6] thermal models. Four steady-state operating conditions corresponding to current levels ranging from approximately one-quarter of the rated current to the rated current of the investigated conductor were considered. Operating conditions exceeding the rated current were excluded from the temperature estimation comparison, as

Table 2. Calculated conductor temperatures for different values of conductor surface emissivity.

Emissivity, ε	**Calculation model**	**Calculated conductor temperature, T_c (°C)**			
		53.39 A	**105.16 A**	**141.56 A**	**181.46 A**
0.90	$R = f(T)$	24.50	36.20	47.80	64.30
	$R = f(T, I)$	24.10	35.60	48.20	66.40
0.51	$R = f(T)$	25.40	39.20	53.00	73.00
	$R = f(T, I)$	24.90	38.40	53.00	74.40
0.30	$R = f(T)$	26.00	41.20	56.40	78.60
	$R = f(T, I)$	25.60	40.50	57.30	82.30

the conductor temperature rapidly approached the 80–100 °C threshold during these tests, preventing the establishment of a well-defined steady state suitable for thermal model validation. The measured operating conditions, experimentally determined conductor parameters, and the corresponding temperature estimation results are summarized in Table 1. For each operating condition, the measured current and ambient temperature, together with the corresponding conductor resistance parameters, were used as input data for the thermal calculations, while the experimentally measured conductor temperature served for model validation. All experiments were conducted under zero-wind conditions, thereby eliminating the influence of forced convective cooling. Under these laboratory conditions, both thermal models produced identical conductor temperature estimates for the conventional ($R = f(T)$) and the proposed ($R = f(T, I)$) resistance models. This equivalence arises because, under zero-wind conditions, forced convective cooling is absent and heat dissipation is governed solely by natural convection and radiation, for which both IEEE Std 738 [6] and CIGRÉ TB 601 [7] adopt equivalent formulations, yielding identical numerical results. Therefore, only one set of calculated temperatures is presented in Table 1.

The results presented in Table 1 show that both resistance models provide satisfactory agreement with the experimentally measured conductor temperatures over the investigated operating range. At lower and intermediate current levels, the differences between the two resistance models are relatively small, with temperature deviations generally below 1.5 °C. However, as the conductor current approaches its rated value, the influence of current-dependent AC resistance becomes more pronounced. Under the highest investigated loading condition, the conventional model underestimates the conductor temperature by approximately 2.3 °C, whereas the proposed model reduces this deviation to less than 1 °C. These results demonstrate that incorporating the experimentally determined current dependence of AC resistance improves the accuracy of conductor temperature estimation under high-load operating conditions, while its influence remains relatively small at lower current levels.

3.3 Influence of Conductor Surface Emissivity at Different Operating Current Levels

In the previous section, conductor temperatures were compared using the experimentally determined surface emissivity of 0.51, identified for the investigated 48-AL1/8-ST1A conductor [2]. To evaluate the sensitivity of conductor temperature estimation to the assumed conductor surface emissivity, additional thermal calculations were performed for emissivity values of 0.3 and 0.9. According to CIGRÉ TB 601 [7], these values are representative of new conductors and weathered conductors that have been in service for one or two years in industrial or heavy agricultural environments, respectively. All remaining operating conditions and conductor parameters were kept unchanged. The corresponding calculated conductor temperatures are summarized in Table 2. For each emissivity value, temperatures were calculated using both the conventional temperature-dependent resistance model, $R = f(T)$, and the proposed current- and temperature-dependent resistance model, $R = f(T, I)$. The experimentally determined emissivity of $\varepsilon = 0.51$, adopted in Section 3.2, was taken as the reference value for evaluating the influence of different emissivity assumptions on conductor temperature estimation.

Figure 4 illustrates the influence of conductor surface emissivity on the calculated conductor temperature for the four investigated operating current levels. The markers denote the reference case corresponding to the experimentally determined emissivity of $\varepsilon = 0.51$.

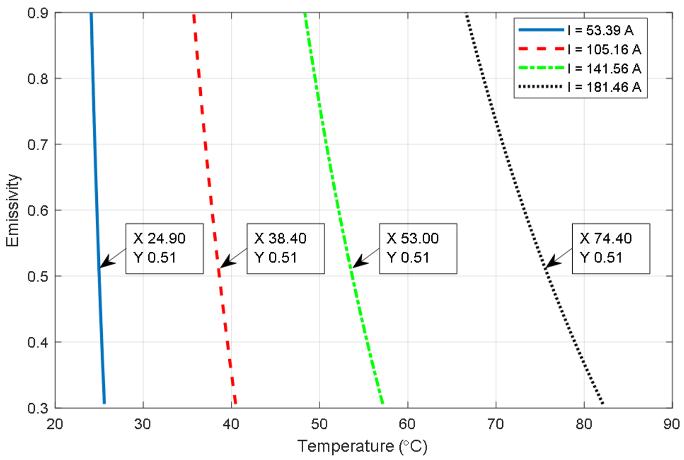

Figure 4. Influence of conductor surface emissivity on the calculated conductor temperature for different operating current levels using the CIGRÉ TB 601 thermal model and the proposed $R = f(T, I)$ resistance model.

The results presented in Table 2 and Figure 4 demonstrate that the conductor surface emissivity has a pronounced influence on the calculated conductor temperature. As expected, increasing the emissivity leads to lower conductor temperatures because of enhanced radiative heat dissipation. Using the calculated temperatures obtained for $\varepsilon = 0.51$ in Section 3.2 as the reference case, Table 2 shows that increasing the emissivity to $\varepsilon = 0.9$ decreases the calculated conductor temperature by approximately 0.9–8.7 °C for the conventional ($R = f(T)$) model and by approximately 0.8–8.0 °C for the proposed ($R = f(T, I)$) model. Conversely, assuming $\varepsilon = 0.3$ increases the calculated conductor temperature by approximately 0.6–5.6 °C for $R = f(T)$ and by approximately 0.7–7.9 °C for $R = f(T, I)$. The difference between the limiting emissivity assumptions, $\varepsilon = 0.3$ and $\varepsilon = 0.9$, becomes particularly pronounced at the highest investigated current level, reaching 14.3 °C for the conventional model and 15.9 °C for the proposed model. Figure 4 further confirms this trend for the proposed $R = f(T, I)$ model, indicating that the influence of surface emissivity on the calculated conductor temperature becomes more pronounced at higher operating currents. As a result, even small variations in surface emissivity lead to progressively larger changes in conductor temperature with increasing conductor loading.

A comparison of the results obtained in Sections 3.2 and 3.3 indicates that, under the investigated operating conditions, conductor surface emissivity has a significantly greater influence on temperature estimation than the current dependence of AC resistance. While incorporating the experimentally determined current-dependent AC resistance improves the temperature prediction by about 2 °C under the highest investigated loading condition, an inappropriate assumption of conductor surface emissivity may change the calculated conductor temperature by more than 15 °C. These findings demonstrate that accurate determination of conductor surface emissivity is essential for reliable conductor temperature estimation and should receive at least the same level of attention as the selection of the electrical resistance model.

4 Conclusions

This paper experimentally investigated the influence of current-dependent AC resistance and conductor surface emissivity on the temperature estimation of a single-layer ACSR conductor. Based on the obtained results, the main conclusions are as follows:

- The experimentally determined AC resistance of the investigated single-layer ACSR conductor depends on both conductor temperature and operating current. The reference AC resistance exhibits a pronounced current dependence, increasing with current due to transformer effects associated with the steel core and approaching saturation at higher current levels.

- Neglecting the current dependence of AC resistance reduces the accuracy of conductor temperature estimation under high-current operating conditions. For the investigated conductor, the conventional temperature-dependent resistance model produced temperature estimation errors of up to approximately 2.5 °C, whereas the use of experimentally determined current-dependent AC resistance reduced the maximum error to less than 1 °C.

- Under the investigated laboratory conditions, identical conductor temperature estimates were obtained using the CIGRÉ TB 601 and IEEE Std 738 thermal models. This indicates that the observed differences originate from the adopted electrical resistance model rather than from the thermal model itself.

- Conductor surface emissivity has a considerably greater influence on temperature estimation than the current dependence of AC resistance. Varying the assumed emissivity from 0.3 to 0.9 resulted in calculated conductor temperature differences exceeding 15 °C, demonstrating that accurate emissivity selection is essential for reliable thermal calculations.

- The obtained results confirm that both experimentally determined AC resistance characteristics and realistic conductor surface emissivity should be considered in conductor thermal analyses and dynamic line rating (DLR) applications. Although the influence of both parameters increases with conductor loading, the sensitivity of the calculated conductor temperature to emissivity is considerably greater than that associated with the adopted AC resistance model.

It should be noted that the presented results were obtained under controlled laboratory conditions with negligible wind, intentionally adopted to isolate the influence of current-dependent AC resistance and conductor surface emissivity on conductor temperature estimation. Therefore, the quantitative results reported in this study should not be directly generalized to all field operating conditions, where convective cooling is governed by environmental factors. Nevertheless, the adopted experimental methodology provides a reliable basis for evaluating the relative influence of the investigated parameters under well-defined operating conditions.

Future work should include experimental investigations under realistic outdoor conditions to validate the proposed approach under different wind speeds and wind attack angles, improve the estimation of convective heat transfer coefficients, and further enhance the accuracy of conductor temperature and ampacity calculations. In addition, more accurate methods for determining conductor surface emissivity under different ageing and environmental conditions should be investigated, given its pronounced influence on conductor temperature estimation demonstrated in this study.

Data Availability Statement

Data will be made available on request.

Funding

This work was supported by the Ministry of Science, Technological Development and Innovation of the Republic of Serbia under Contract No. 451-03-34/2026-03/200155.

Conflicts of Interest

Miloš J. Milovanović served as an Associate Editor of the *ICCK Transactions on Electric Power Networks and Systems* at the time of manuscript submission. To ensure the integrity of the peer-review process, Miloš J. Milovanović was not involved in the editorial handling, peer review, or decision-making process for this manuscript, which was handled independently by another editor. The remaining authors declare no conflicts of interest.

AI Use Statement

The authors declare that no generative AI was used in the preparation of this manuscript.

Ethical Approval and Consent to Participate

Not applicable.

References

[1] CIGRE Working Group 22.12. (2002). *Thermal behaviour of overhead conductors* (Technical Brochure 207). Paris, France: CIGRE. Retrieved from https://www.e-cigre.org/publications/detail/207-thermal-behaviour-of-overhead-conductors.html

[2] Milovanović, M., Jovanović, A., Banjanin, M., Vukašinović, I., Gvozdić, B., Žorić, A., ... & Vukašinović, J. (2026). Experimental Verification of IEEE, CIGRÉ and IEC Thermal Models for Dynamic Line Rating of ACSR Overhead Lines. *Electricity*, *7*(2), 34. [CrossRef]

[3] Fernandez, E., Albizu, I., Bedialauneta, M. T., Mazon, A. J., & Leite, P. T. (2016). Review of dynamic line rating systems for wind power integration. *Renewable and Sustainable Energy Reviews*, *53*, 80-92. [CrossRef]

[4] Abas, N. H., Ab Kadir, M. Z. A., Azis, N., Jasni, J., Ab Aziz, N. F., & Khurshid, Z. M. (2024). Optimizing grid with dynamic line rating of conductors: A comprehensive review. *IEEE Access*, *12*, 9738-9756. [CrossRef]

[5] CIGRE Working Group B2.12. (2008). *Alternating current (AC) resistance of helically stranded conductors* (CIGRE Technical Brochure No. 345). Paris, France: CIGRE. Retrieved from https://www.e-cigre.org/publications/detail/345-alternating-current-ac-resistance-of-helically-stranded-conductors.html

[6] IEEE Standards Association. (2023). *IEEE standard for calculating the current-temperature relationship of bare overhead conductors* (IEEE Std 738-2023, Revision of IEEE Std 738-2012). Piscataway, NJ: IEEE. [CrossRef]

[7] CIGRE Working Group B2.43. (2014). *Guide for thermal rating calculations of overhead lines* (Technical Brochure No. 601). Paris, France: CIGRE. Retrieved from https:

//www.e-cigre.org/publications/detail/601-guide-for-thermal-rating-calculations-of-overhead-lines.html

[8] International Electrotechnical Commission. (2021). *Overhead electrical conductors – Calculation methods for stranded bare conductors* (IEC TR 61597:2021). Geneva, Switzerland: IEC. Retrieved from https://webstore.iec.ch/en/publication/61412

[9] Riba, J. R. (2024). The role of AC resistance of bare stranded conductors for developing dynamic line rating approaches. *Applied Sciences, 14*(19), 8982. [CrossRef]

[10] Meyberg, R. A., Absi Salas, F. M., Domingues, L. A. M., Sens, M. A., Correia de Barros, M. T., & Lima, A. C. (2021). Magnetic properties of an ACSR conductor steel core at temperatures up to 230°C and their impact on the transformer effect. *IET Science, Measurement & Technology, 15*(2), 143-153. [CrossRef]

[11] Morgan, V. T. (2013). The current distribution, resistance and internal inductance of linear power system conductors—A review of explicit equations. *IEEE Transactions on Power Delivery, 28*(3), 1252-1262. [CrossRef]

[12] Riba, J. R., Liu, Y., Moreno-Eguilaz, M., & Sanllehí, J. (2022). On-line core losses determination in ACSR conductors for DLR applications. *Materials, 15*(17), 6143. [CrossRef]

[13] Xie, D., Qin, Z., Xie, S., Jiang, J., Bai, F., Li, J., & He, G. (2024). Research on the measurement of AC resistance of overhead transmission lines considering actual operating conditions. *Energies, 17*(24), 6336. [CrossRef]

[14] Riba, J. R., Liu, Y., & Moreno-Eguilaz, M. (2024). Analyzing the role of emissivity in stranded conductors for overhead power lines. *International Journal of Electrical Power & Energy Systems, 159*, 110027. [CrossRef]

[15] Milovanović, M. J., Perović, B. D., & Radosavljević, J. N. (2025, June). Development of a LabVIEW-Based Experimental System for Measuring Electrical and Thermal Characteristics of ACSR Conductors. In *2025 14th Mediterranean Conference on Embedded Computing (MECO)* (pp. 1-6). IEEE. [CrossRef]

[16] Joint Committee for Guides in Metrology. (2008). *Evaluation of measurement data – Guide to the expression of uncertainty in measurement* (JCGM 100:2008). Sèvres, France: Bureau International des Poids et Mesures. Available at https://www.bipm.org/documents/20126/2071204/JCGM_100_2008_E.pdf

Miloš J. Milovanović received his B.Sc., M.Sc., and Ph.D. degrees in Electrical and Computer Engineering from the Faculty of Technical Sciences, University of Priština in Kosovska Mitrovica, in 2013, 2015, and 2021, respectively. He is currently an Associate Professor in the Department of Power Engineering at the same faculty. His research interests include power system analysis and optimization, power quality, electrical measurements, and distributed power generation. He has authored or co-authored over 60 journal and conference papers, with more than 500 citations and an h-index of 13. (Email: milos.milovanovic@pr.ac.rs)

Andrijana D. Jovanović received her B.Sc. and M.Sc. degrees in Electrical and Computer Engineering from the Faculty of Technical Sciences, University of Priština in Kosovska Mitrovica, in 2020 and 2022, respectively. She is an Assistant in the Department of Power Engineering at the same faculty. Her research interests include dynamic line rating of overhead transmission lines, thermal and electrical modeling of ACSR conductors, electrical measurements, data acquisition systems, and power system monitoring. (Email: andrijana.jovanovic@pr.ac.rs)

Bojan D. Perović received his B.Sc., M.Sc., and Ph.D. degrees in Electrical and Computer Engineering from the Faculty of Technical Sciences, University of Priština in Kosovska Mitrovica, in 2011, 2012, and 2018, respectively. He is currently an Associate Professor in the Department of Power Engineering at the same faculty. His research interests include renewable energy sources and power cable systems. He has authored or co-authored over 50 journal and conference papers, with more than 300 citations and an h-index of 11. (Email: bojan.perovic@pr.ac.rs)